

Why does the second peak of pair correlation functions split in quasi-two-dimensional disordered films?

K. Zhang, H. Li, L. Li, and X. F. Bian

Citation: [Appl. Phys. Lett.](#) **102**, 071907 (2013); doi: 10.1063/1.4793187

View online: <http://dx.doi.org/10.1063/1.4793187>

View Table of Contents: <http://apl.aip.org/resource/1/APPLAB/v102/i7>

Published by the [AIP Publishing LLC](#).

Additional information on Appl. Phys. Lett.

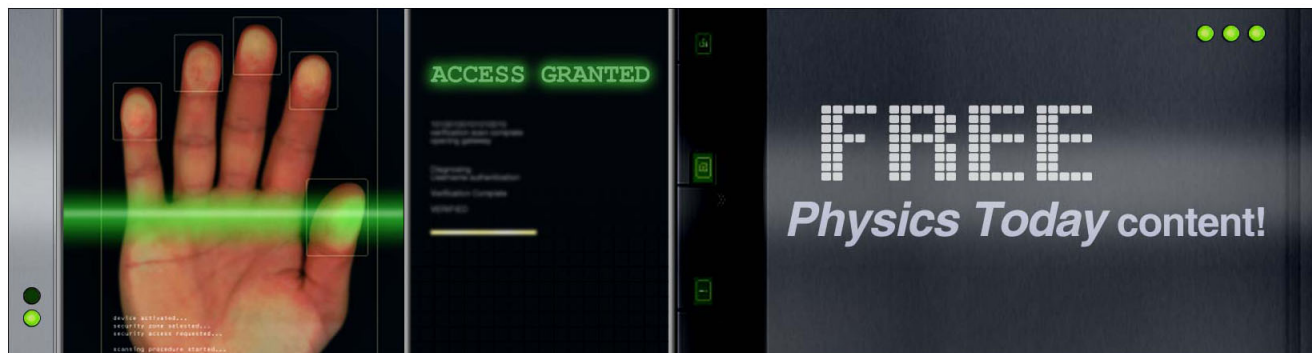
Journal Homepage: <http://apl.aip.org/>

Journal Information: http://apl.aip.org/about/about_the_journal

Top downloads: http://apl.aip.org/features/most_downloaded

Information for Authors: <http://apl.aip.org/authors>

ADVERTISEMENT



Why does the second peak of pair correlation functions split in quasi-two-dimensional disordered films?

K. Zhang,¹ H. Li,^{1,a)} L. Li,^{2,b)} and X. F. Bian¹

¹Key Laboratory for Liquid-Solid Structural Evolution and Processing of Materials, Ministry of Education, Shandong University, Jinan 250061, People's Republic of China

²The Institute of Textiles and Clothing, The Hong Kong Polytechnic University Hung Hom, Kowloon, Hong Kong

(Received 3 December 2012; accepted 5 February 2013; published online 21 February 2013)

Molecular dynamics simulation has been performed to study the splitting of the second peak in pair correlation functions of quasi-two-dimensional disordered film. A quasi-two-dimensional inhomogeneous structural model, which contains both crystal-like and disordered regions, supports the hypothesis that the splitting of the second peak is result of a statistical average of crystal-like and disordered structural regions in the system, not just the amorphous structure. The second-peak splitting can be viewed as a prototype of the crystal-like peak exhibiting distorted and vestigial features. © 2013 American Institute of Physics. [<http://dx.doi.org/10.1063/1.4793187>]

Ultrathin disordered metal films with a thickness of one or a few monolayers attract much attention, since they are now available as epitaxial films on insulating substrates and are, therefore, the best model systems for two-dimensional (2D) conduction in metal systems.¹ Disorder is known to play an important role in the phase diagram of the superconductor material at low temperatures and high magnetic fields.² Significant effort is currently being invested in attempting to understand theoretically the interplay between disorder and the conductivity in 2D systems.^{3–5} Semiconductor technology requires thinner and thinner films, so that the properties due to restriction to thicknesses of a few monolayers become also technological importance. Since the detailed atomic structure and the restriction to a thickness smaller than the bulk mean free path may modify the physical and chemical properties dramatically, study of the disordered film becomes valuable in material science and physics.^{6–8} Huang *et al.* reported the accidental discovery of 2D amorphous silica supported on graphene.⁹ They found that the images of 2D amorphous silica contain both the crystalline and amorphous regions. Lichtenstein *et al.* studied the interface between a crystalline and amorphous phase of silica film supported by the Ru(0001) substrate.¹⁰ The atomic structure of the topological transition from a crystalline to an amorphous phase in the thin silica film can lead to a better description of the crystal-to-glass and the liquid-to-glass transitions. Although there has been much progress in the understanding of the properties of amorphous materials in three-dimension,^{11–13} some important questions on the microstructural feature and its forming mechanism of the 2D disordered films have remained unanswered.^{14–16} Therefore, further studies on the atomic structures of the 2D disordered systems and their physical proprieties are necessary. In general, pair correlation function (PCF) methods can provide a useful way to accurately estimate the mass density of thin layers of amorphous materials, which serves as a key test for the structural models of 2D amorphous materials. It also yields central information reflected by the short-range

order and medium-range order, i.e., it makes it possible to obtain the global structural information on the atomic structure of 2D systems at different length scales.

A splitting of the second peak in the PCF curve in three-dimensional materials is usually regarded as a characteristic indication of disordered structure forming.^{17,18} However, owing to the lack of one dimensionality as well as the difference of atomic arrangement, the explanation on the second peak of the PCF in 2D systems should be clarified. In addition, previous studies are usually based on the viewpoint of how the clusters connect to each other to form a large supercluster with a specific geometric structure. Due to the fact that the PCF is the statistical average of the atomic configuration, it seems more appropriate to use the statistical methods to interpret the nature of the splitting of the second peak in the PCF in 2D system. Actually, fewer efforts have focused on the relation between the splitting of the second peak and the crystalline or glass formation of 2D disordered films by statistical average analysis. This unsatisfactory state has hindered not only the evaluation criteria of amorphous materials but also the clarification of the mechanism of the liquid-glass transition. Disordered structures are usually obtained by rapid cooling process. In order to understand these questions well, it is necessary to investigate the structural evolution of liquid-glass transition. 2D film system is believed to be convenient to monitor the global structural information in the liquid-glass transition.^{19,20} Therefore, the main purpose of this study is, using molecular dynamics (MD) simulation, to provide a statistical explanation on the nature of the splitting of the PCF in the 2D system.

Simulations were performed using the embedded atom method (EAM) potential²¹ supplied in LAMMPS.²² A system with 6400 Cu atoms distributed in a $20 \times 20 \times 1$ lattice unit box was employed to model the quasi-two-dimensional Cu. Periodic control was exerted on the x- and y-directions of the box, and the z-direction was nonperiodic. Specially, the lower boundary of the simulation box along the z-direction (not refer to atoms) was fixed, while the upper boundary was free. That was to say, a virtual wall was set at the lower edge of the simulation box in the z-direction, which is similar to

^{a)}Electronic mail: lihuilmy@hotmail.com.

^{b)}Electronic mail: tclili@inet.polyu.edu.hk.

the substrate in experiment.²² The initial box lattice was set to 3.61 Å, and the initial positions of the atoms were arranged in the light of the fcc crystal structure. The MD time step was chosen as 1 fs. The temperature was controlled by a Nose-Hoover thermostat.²³ First, the well-equilibrated liquid was prepared by gradually heating the ideal crystal from 1 to 1800 K at a low heating rate, then relaxing it at 1800 K for 30 ps. Next, the liquid system was quenched to $T = 300$ K at different cooling rates, varying from 10 to 500 K/ps. At each given temperature, the atomic configurations were recorded for further analysis.

The PCFs of the quasi 2D Cu are shown in Fig. 1. It is worth noting that the main peak height of the PCFs, which represents the nearest-neighbor shell, increases significantly with the decreasing temperature, and the second peak begins to split. As shown in Figs. 1(a) and 1(b), at the cooling rates of $Q1 = 500$ K/ps and $Q2 = 250$ K/ps, the second peak begins to split into two subpeaks at 633 K. Interestingly, a small shoulder peak appears between the first and second peaks at 300 K in Fig. 1(b), which means the short- or medium-range ordered structures form. With the cooling rate decreasing to $Q3 = 100$ K/ps, the splitting emerges at 800 K; moreover, the small shoulder peak between the first and second peaks arises on the left at 300 K with significant height, which indicates that the length of the ordered structure is further extended to a large scale. At the cooling rate of $Q4 = 10$ K/ps, the left shoulder peak arises at 633 K and becomes more prominent than the right subpeak as the temperature decreases, suggesting that the orientation of the crystalline structure becomes more consistent. It is widely known that the atomic structure of amorphous materials is similar to that of liquid metals, and the fact that the second peak of the PCFs splits into two subpeaks is regarded as a characteristic indication of disordered structures. However, this is not the true case in two-dimensional systems. As shown in Figs. 1(c) and 1(d), the evolution of the PCFs clearly indicates how the second-peak splitting converts into crystal peaks. For example, as shown in Fig. 1(d), at 800 K, the splitting of the second peak of the PCF appears, but at 633 K, the splitting of the second peak

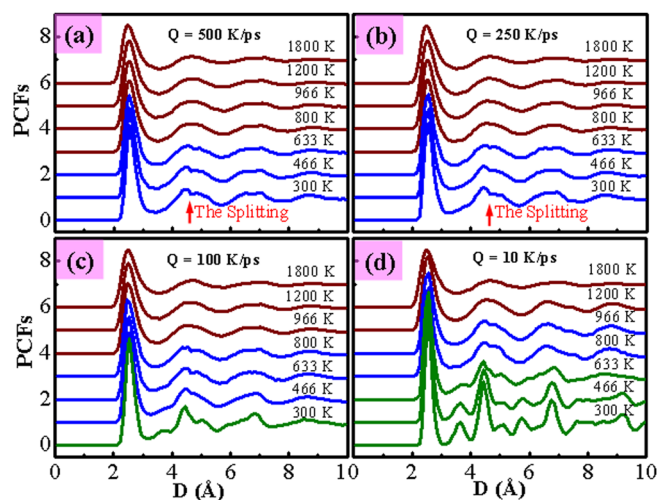


FIG. 1. PCFs of the quasi 2D Cu during cooling with four different cooling rates (i.e., 500, 250, 100, and 10 K/ps). The brown curve represents the PCF without the splitting of the second peak, the blue represents that with the splitting of the second peak, and the green is the typical crystal peak.

becomes three peaks, and finally these three peaks evolve into three typical crystal peaks at 466 K. Based on this evolution trend, it can be seen that the splitting second-peak has a close relationship with crystal peak, and that the splitting second-peak is the rudiment of the crystal peaks. Our simulations do not support other hypothesis which states that the splitting of the second peak occurs as a result of the connection of some small clusters to a supercluster with a special geometrical structure.

In order to further clarify the origin of the splitting of the second peak, the structural configuration of the quasi 2D Cu at 300 K at the cooling rate of $Q2 = 250$ K/ps is supplied in Fig. 2. The LAMMPS software²² defines a computation that calculates the common neighbor analysis (CNA) pattern for each atom in the group,^{24,25} which is described according to the Honeycutt and Andersen bond analysis.²⁶ In solid-state systems, the CNA pattern is a useful measure of the local crystal structure around an atom. Generally, there are five kinds of CNA patterns that LAMMPS recognizes, which are defined as follows: fcc = 1, hcp = 2, bcc = 3, icosohedral = 4, and unknown = 5. The first three indices are all “crystalline.” Also note that the CNA calculation in LAMMPS uses the neighbors of an owned atom to find the nearest neighbors of a ghost atom. It is seen that the overall atomic structure consists of two types of regions: the well-organized region with crystal-like order and the fully disordered region with some packing frustration. Our theoretical results are in good agreement with the experiments by Huang and Lichtenstein,^{9,10} which prove our MD simulation result is reliable. It is also worth noting that in the disordered region there are some single strings, arcs, and rings which clearly illustrate the packing frustration of the atoms in the quick cooling process. In fact, Fig. 2(a) shows that the structure of the quasi 2D amorphous Cu is the mixture of crystal-like and fully disordered structural regions with a certain percentage. The local PCFs in these two distinct regions differ from one another. As shown in Figs. 2(b)–2(d), the local PCFs of the crystalline region have some crystal-like subpeaks, showing typical crystalline features, while the local PCFs in the fully disordered structural region show no splitting on the second peak. However, the global PCFs averaged by the overall atomic structures of

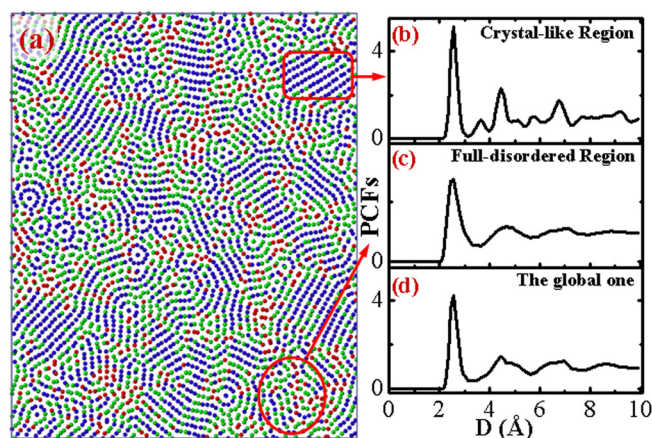


FIG. 2. (Left) Local atomic arrangement of the quasi 2D Cu at 300 K with the cooling rate of $Q2 = 250$ K/ps. Blue: atoms with crystal-like ordering; others: fully disordered ordering. (Right) From top to bottom: PCF curves of the local crystal-like region, fully disordered region and global region.

the two types of regions show a slight splitting in the second peak. It is known that the PCF is the statistical average of the structural configuration, thus, the slight splitting of the global PCF is caused by the combined average results of the crystal-like and fully disordered regions. Moreover, the very similar results are also obtained for the simulations of the quasi 2D Co, which indicate the coexistence of crystal-like and fully disordered regions. The splitting of the second peak in 2D systems may not be the signature of the glass formation, but the appearance of both the crystal-like and disordered structures. The splitting second-peak can be viewed as an embryonic form of the crystal peak.

The above results arouse us to further investigate the origin of these two subpeaks in the second-peak splitting. Fig. 3 shows the respective PCF curves of the liquid, amorphous, and ideal crystalline solid Cu. It is known that in ideal fcc crystal there are four nearest coordinated shells, namely, $R_1 = 2.55 \text{ \AA}$, $R_2 = 3.61 \text{ \AA}$, $R_3 = 4.44 \text{ \AA}$, and $R_4 = 5.12 \text{ \AA}$. The positions of the first peak in both the liquid and amorphous Cu correspond to the ones in the ideal fcc crystal at $R_1 = 2.55 \text{ \AA}$, while the second peaks correspond to three peaks of the ideal fcc crystal at the locations $R_2 = 3.61 \text{ \AA}$, $R_3 = 4.44 \text{ \AA}$, and $R_4 = 5.12 \text{ \AA}$. From the correspondence of the peak positions and the evolution trend, it is concluded that the two subpeaks on the second peak are due to the appearance of a small amount of the short-or medium-range ordered structures.

Fig. 4 shows the fraction of the crystal-like regions with the temperature at different cooling rates. If the splitting occurs on the right without the left subpeak, this point is labeled with a blue arrow, while if both the left and right subpeaks appear, it is labeled with a red arrow. According to this rule, Fig. 4 may be divided into three zones. When the fraction of the crystal-like region is less than 18.5%, it belongs to the non-splitting region corresponding to the fully disordered structure in the liquid state. If the fraction of crystal-like region exceeds to 50%, the left shoulder subpeak appears, which indicates it almost becomes the polycrystalline structure. However, if the fraction ranges from 18.5% to 50%, it is the mixture of the disordered and crystal-like structural regions, which results in the splitting second peak

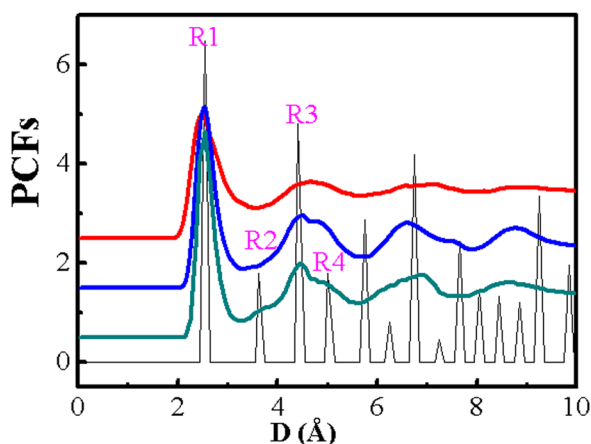


FIG. 3. PCF curves of the liquid, amorphous, and ideal crystal Cu; red line: liquid Cu at 1800 K; blue line: solid Cu at 300 K (cooling rate: $Q = 400 \text{ K/ps}$); green line: solid Cu at 300 K (cooling rate: $Q = 200 \text{ K/ps}$); black line: ideal crystal Cu. R_1 , R_2 , R_3 , and R_4 represent the ideal fcc peaks, respectively.

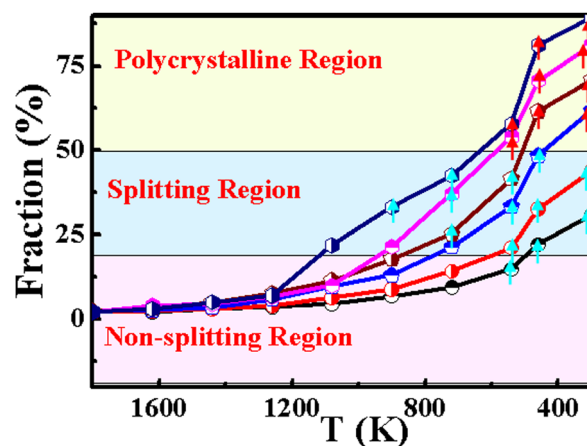


FIG. 4. Relationship between the fraction of the crystal-like region and the splitting of the second peak with different cooling rates: black line: 500 K/ps; red line: 250 K/ps; blue line: 100 K/ps; brown line: 50 K/ps; purple line: 25 K/ps; and dark blue line: 10 K/ps.

of the PCF. The disordered structure in two-dimension may be a simple mixture of crystal-like and fully disordered region, which sheds a new light on the understanding of the atomic structure of the low-dimensional materials.

In summary, the origin of the splitting of the second peak in PCFs is a statistical result of the disordered and crystal-like ordered structure with a certain percentage rather than the fully disordered structure. The results show that the shoulder peak on the left side of the second peak is due to the appearance of a small amount of the short-or medium-range ordered structures. The structure in 2D disordered film may be a simple mixture of the crystal-like and disordered structural regions. These findings provide physical and dynamic insights into the solidification feature of the quasi 2D systems.

The authors would like to acknowledge the support provided by the National Basic Research Program of China (Grant No. 2012CB825702). This work was also supported by the National Natural Science Foundation of China (Grant Nos. 51271100 and 50831003).

- ¹O. Pfennigstorf, A. Petkova, H. L. Guenter, and M. Henzler, *Phys. Rev. B* **65**, 045412 (2002).
- ²N. K. Wilkin and H. J. Jensen, *Phys. Rev. Lett.* **79**, 4254–4257 (1997).
- ³M. Strongin, R. S. Thompson, O. F. Kammerer, and J. E. Crow, *Phys. Rev. B* **1**, 1078–1091 (1970).
- ⁴A. Ulman, *Chem. Rev.* **96**, 1533–1554 (1996).
- ⁵O. Crauste, F. Couedo, L. Berge, C. Marrache, and L. Dumoulin, *J. Phys.: Conf. Ser.* **400**, 022012 (2012).
- ⁶J. C. Meyer, C. O. Girit, M. F. Crommie, and A. Zettl, *Nature* **454**, 319–322 (2008).
- ⁷Z. Y. Zheng, F. Wang, and Y. L. Han, *Phys. Rev. Lett.* **107**, 065702 (2011).
- ⁸M. J. Cliffe, M. T. Dove, D. A. Drabold, and A. L. Goodwin, *Phys. Rev. Lett.* **104**, 125501 (2010).
- ⁹P. Y. Huang, S. Kurasch, A. Srivastava, V. Skakalova, J. Kotakoski, A. V. Krashennnikov, R. Hovden, Q. Mao, J. C. Meyer, J. Smet *et al.*, *Nano Lett.* **12**, 1081 (2012).
- ¹⁰L. Lichtenstein, M. Heyde, and H. J. Freund, *Phys. Rev. Lett.* **109**, 106101 (2012).
- ¹¹J. D. Bernal, *Nature* **183**, 141 (1959).
- ¹²P. H. Gaskell, *Nature* **276**, 484 (1978).
- ¹³D. Levine and P. J. Steinhardt, *Phys. Rev. Lett.* **53**, 2477 (1984).

- ¹⁴D. Loffler, J. J. Uhlrich, M. Baron, B. Yang, X. Yu, L. Lichtenstein, L. Heinke, C. Buchner, M. Heyde, S. Shaikhutdinov *et al.*, *Phys. Rev. Lett.* **105**, 146104 (2010).
- ¹⁵P. Y. Huang, C. S. Ruiz-Vargas, A. M. van der Zande, W. S. Whitney, M. P. Levendorf, J. W. Kevek, S. Garg, J. S. Alden, C. J. Hustedt, Y. Zhu *et al.*, *Nature* **469**, 389 (2011).
- ¹⁶X. Yu, B. Yang, J. A. Boscoboinik, S. Shaikhutdinov, and H. J. Freund, *Appl. Phys. Lett.* **100**, 151608 (2012).
- ¹⁷D. Ma, A. D. Stoica, and X. L. Wang, *Nature Mater.* **8**, 30 (2009).
- ¹⁸C. H. Bennett, *J. Appl. Phys.* **43**, 2727 (1972).
- ¹⁹K. Watanabe and H. Tanaka, *Phys. Rev. Lett.* **100**, 158002 (2008).
- ²⁰K. Zhang, Y. Y. Jiang, H. Li, P. C. Si, Y. F. Li, H. Q. Yu, K. M. Liew, and X. G. Song, *Europhys. Lett.* **96**, 46005 (2011).
- ²¹X. W. Zhou, *Acta Mater.* **49**, 4005 (2001).
- ²²S. J. Plimpton, *J. Comp. Phys.* **117**, 1 (1995).
- ²³S. J. Nose, *J. Chem. Phys.* **81**, 511 (1984).
- ²⁴D. Faken and H. Jonsson, *Comput. Mater. Sci.* **2**, 279 (1994).
- ²⁵H. Tsuzuki, P. S. Branicio, and J. P. Rino, *Comput. Phys. Commun.* **177**, 518 (2007).
- ²⁶J. D. Honeycutt and H. C. Andersen, *J. Phys. Chem.* **91**, 4950–4963 (1987).